ELSEVIER

Ceramics International 25 (1999) 631–637

CERAMICS INTERNATIONAL

Characterization of vapour deposited products in furnace tube during SiC synthesis from carbonized rice hulls

Hsiung-Wen Han*, Hok-Shing Liu

Department of Mineral and Petroleum Engineering, National Cheng Kung University, Tainan, Taiwan

Received 12 March 1998; received in revised form 4 July 1998; accepted 1 September 1998

Abstract

The vapour deposited products on graphite substrates in the cold zone (1270–600°C) for the preparation of SiC from carbonized rice hulls (CRH) in a vacuum tube furnace, which is operated at a reacting sample chamber temperature of 1300°C, have been characterized by various analytical techniques, such as SEM/EDS, XRD, FTIR, XPS and AES. Morphology/size, chemical composition, lattice/electronic structure, and molecular vibration modes of these products have been obtained. The primary deposited product in zone A (1270–1050°C) was a thin film, consisting of SiO_xC_y and SiC; in zone B (1050–820°C) were whiskers aggregates, consisting of crystalline Si and amorphous SiO_2; in addition, in zone C (820–600°C) spheroids aggregates have been observed consisting of amorphous Si and SiO_2. The morphology sequence of the deposits in the cold zone, e.g. the thin film (SiO_xC_y/SiC)→whiskers (Si/SiO_2)→spheroids (Si/SiO_2), seem to be related to the substrate temperature and degree of supersaturation of the reacting gas (SiO).

Keywords: Carbonized rice hulls (CRH); Vapour deposited product; Reaction zone; Cold zone; SiO_xC_y; SiC; Chemical vapour deposition (CVD)

1. Introduction

There have been substantial studies on the preparation of silicon carbide (SiC) whiskers from various forms of rice hulls, such as raw rice hulls (containing 15–20 wt% of silica) [1–4], rice hull ashes [5,6], and carbonized rice hulls (CRH) [7–9]. Basically the process consists of the raw materials reacting with or without additives of carbon and iron catalyst at a temperature range of 1300–1600°C in a vacuum furnace or in an inert or reducing atmosphere (Ar, N_2, H_2, etc.). Previous studies [10–16] focus primarily on reaction mechanism and kinetics, conversion efficiency, microstructure, crystal chemistry, and morphology of SiC products from rice hulls. Despite these efforts, the various vapour deposits [17–19], e.g. silicon oxycarbide (SiO_xC_y) and SiC whiskers, which were deposited by a vapour-phase reaction over an area of the reactor tube wall at around 1200°C, compared with 1500°C as the reaction temperature of CRH, have seldom been evaluated. A relevant task is to study the vapour deposited products on the reactor tube wall at a lower temperature range (the cold zone), i.e. between 1270 and 600°C, when the reaction temperature of CRH is 1300°C. These deposits may be highly promising for industrial applications and may increase the commercial values of CRH conversion towards SiC.

The major mechanisms [6,19] in the conversion of SiC from rice hulls can be represented by the following equations:

$$SiO_{2(s)} + C_{(s)} \rightarrow SiO_{(g)} + CO_{(g)} \quad (1)$$

$$SiO_{2(s)} + CO_{(g)} \rightarrow SiO_{(g)} + CO_{2(g)} \quad (2)$$

$$SiO_{(g)} + 2C_{(s)} \rightarrow SiC_{(s)} + CO_{(g)} \quad (3)$$

$$SiO_{(g)} + 3CO_{(g)} \rightarrow SiC_{(s)} + 2CO_{2(g)} \quad (4)$$

Notably, the above reactions are inevitable for producing SiO, CO and CO_2 gases. These gases may react with each other or the tube wall, or deposit on the cold wall when they flow through the reactor tube to the furnace outside. The reactions imply that different reaction products may be separately formed in different temperature zones of the reactor tube, namely: (1) raw material sample chamber for CRH (reaction zone, the highest temperature) and (2) the cold zone (outside reaction zone).

* Corresponding author. Tel.: +886-37-355028-15; fax: +886-37-324047.

0272-8842/99/$ - see front matter
PII: S0272-8842(98)00077-7

The purpose of this study is to characterize the different vapour deposited products in the cold zone between 1270 and 600°C, when CRH is in the reaction zone of tube furnace at 1300°C. SEM/EDS, XRD, FTIR, XPS and AES techniques have been used to analyze the morphology/surface texture, chemical composition, crystalline phase, molecular vibration modes, and electronic structures of the different deposits in the reactor tube.

2. Experimental procedure

The raw materials used in this study were black granular carbonized rice hulls (CRH), which were prepared by partial pyrolysis of the raw rice hulls at about 700°C in a rotary kiln. Using an elementary analyzer (Heraeus Co.) for C/H/O, the test materials were shown to contain (wt) 48.96% C; 1.67% H_2; 8.39% O_2; and 40.98% ash. Based on ICP-AES (Jarrel-Ash, ICAP 9000) analysis, the ash components were (wt) 93.92% SiO_2; 0.32% Al_2O_3; 0.16% Fe_2O_3; 0.17% MnO; 0.5% MgO; 1.25% CaO; 3.46% K_2O; and 0.2% Na_2O. CRH had a BET specific surface area of 200 $m^2 g^{-1}$.

A sketch of the reactor system is shown in Fig. 1. It consists of a double-tube structure, i.e. an outer Al_2O_3 tube, $\phi 6\times 100$ cm, protected by an inner graphite tube, $\phi 5\times 60$ cm. The CRH (approximately 2g) was placed in a $4\times 10\times 2$ cm boat-like graphite sample chamber. Next, 12 pieces of rectangular graphite substrates, $2\times 1\times 0.2$ cm each, were placed into the cold zone of reactor tube and adjacent to the sample chamber. The graphite substrates were chosen to receive the vapour deposited products from the gases of CRH in the reaction zone at 1300°C because analyzing the deposits on the substrate was easier than on the tube wall. The total temperature drop in the cold zone was 700°C, i.e. from 1300°C for the reacting chamber to 600°C for the farthest substrate.

The reacting system was operated under a vacuum condition, controlled at 6.67 Pa (5×10^{-2} torr) by a vacuum pump. The temperature distribution in the reacting chamber and the cold zone of the tube furnace was measured by a thermocouple before the experimental run. Temperature was elevated at a rate of 5°C min^{-1} to 1300°C, and kept for 60 min. After cooling to room temperature, the graphite substrates were taken out of the furnace for subsequent analytical works.

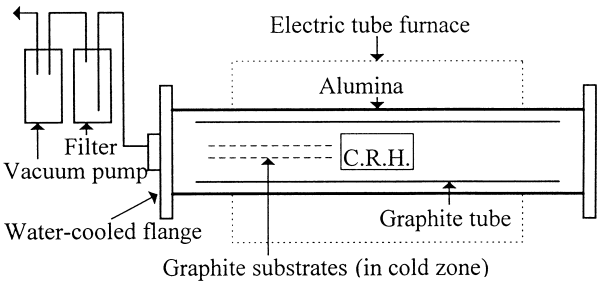

Fig. 1. Sketch of double-tube vacuum furnace apparatus.

The morphologies of deposits were observed by scanning electron microscope (SEM, Hitachi S-4100). The chemical compositions of deposits were determined by using an ultra-thin window energy dispersive X-ray spectrometer (EDS, Noran) attached on SEM. X-ray powder diffraction patterns were obtained by using an X-ray diffractometer (XRD, Rigaku D-2200). Infrared diffuse reflection spectra (DRIFT) of deposits were taken over a range of 4000–400 cm^{-1} using a Fourier transform infrared spectrometer (FTIR, Jasco 300E). X-ray photoelectron spectrometer (XPS, Fisions Lab-210) excited with a Mg Kα (1253.6 eV) X-ray source was used to characterize the chemical bonding of the deposits. Compositions of depth profile were obtained by an Auger electron spectrometer (AES, Fisions 310D).

3. Results and discussion

3.1. In-situ products of the sample chamber (1300°C)

The primary conversion of CRH into SiC was performed in the sample holding chamber in which the reacting temperature was maintained at 1300°C. The products were β-SiC and low cristobalite (SiO_2) identified by XRD, as shown in Fig. 2(b). CRH was an amorphous phase before reaction [Fig. 2(a)]. Obviously, the raw materials did not react completely at 1300°C so SiO_2 and carbon residuals appeared on XRD pattern.

3.2. Deposits on graphite substrates in the cold zone (1270–600°C)

Twelve pieces of graphite substrates were extracted from the cold zone after CRH reacted in reaction zone at 1300°C. Next, the vapour deposited products on each

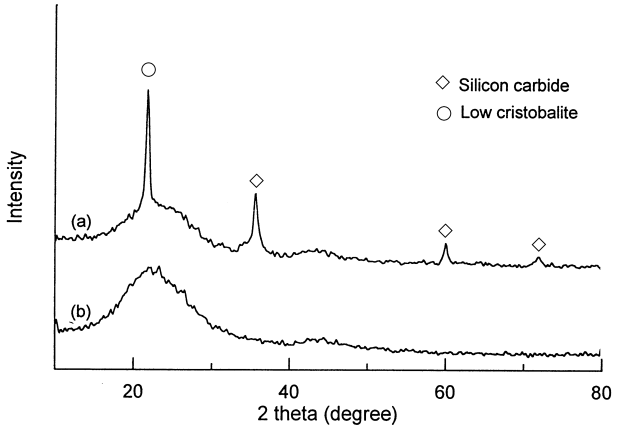

Fig. 2. X-ray diffractograms of (a) products of heat-treated CRH in vacuum at 1300°C and (b) carbonized rice hulls (CRH).

graphite substrate section were carefully examined and analyzed. As presented in Table 1, the deposits had three kinds of morphology which were related to substrate temperature and position: (1) the thin film was in zone A, 1270–1050°C; (2) whiskers aggregates were in zone B, 1050–820°C; and (3) spheroids aggregates were in zone C, 820–600°C. Experimental results obtained from deposits are described in the following.

3.2.1. SEM/EDS morphology and chemical analysis

Fig. 3 displays the SEM photographs and EDS results of deposits on the graphite substrates. Each micrograph is briefly described as follows: The thin film deposit in zone A appeared to have major elements of Si and C, as shown in Fig. 3(a). There was no Si element to be detected above 1270°C by EDS and XPS, and the quantity of Si element tended to increase with decreasing temperature in this zone. On SEM photograph, the deposit's morphology was vague but graphite particles of substrate could be observed clearly. Being heat-treated in air at 800°C for 1 h, the graphite substrate was burned off completely and a white yellowish thin film remained. Therefore, it can be assumed that the deposit on graphite substrate of this zone is a transparent thin film. The whiskers (zone B), 1–6 μm in length and about 0.1 μm in diameter, had a major elements Si and O, as shown in Fig. 3(b). The size of whiskers became larger with decreasing substrate temperature. In zone C the spheroids which seemed to be composed of small submicron particles as nuclei, had major elements Si and O, as Fig. 3(c) shows. Moreover, in this zone, the diameter of spheroids were around 0.6–2 μm and increased with temperature.

3.2.2. Deposits phases by XRD analysis

Glazing incident X-ray diffraction (GIXD) patterns of the thin film, whiskers and spheroids deposits are shown in Fig. 4. It was revealed that most of the strong peak intensity belonged to the graphite phase ($2\theta = 26.5$, 42.6, 44.5, 54.6, 77.7°) of substrate, SiC crystalline phase ($2\theta = 35.7$, 60.1°) was observed among the thin film, in addition, Si crystalline phase ($2\theta = 28.5$, 47.3, 56.1°) appeared in the whiskers, as Fig. 4(a) and (b) show, respectively. Notably, no crystallite was formed among the spheroids except graphite phase, as shown in Fig. 4(c). To realize the amorphous phase in zone C, the deposits were separately heated at 1000 and 1200°C for 1 h in a vacuum furnace; and, respectively, crystalline silicon and low cristobalite (SiO_2) were subsequently identified by XRD diffractograms in Fig. 5(a) and (b). According to Blanchard and Schunb [20], Si crystallite appears to form around 900°C for the pyrolytic conversion of perhydropolysilazane into Si_3N_4. Thus, the spheroids and whiskers represent a mixture of Si and SiO_2, presumably to have been formed by the decomposition reaction of amorphous solid SiO to Si and SiO_2 on the graphite substrates at a lower temperature (below 1100°C) [21,22], as the following:

$$2SiO_{(am)} \rightarrow SiO_{2(s)} + Si_{(s)} \quad (5)$$

Therefore, the phases of different deposits in the cold zone appear to be related to the substrate temperature and position, such as SiC crystallite in zone A, Si crystallite and amorphous SiO_2 in zone B, and amorphous Si and SiO_2 in zone C.

Table 1
Vapour deposited products in the cold zone differentiated by temperature and position of graphite substrates

Zones	A	B	C
Temperature, °C	1270 ←—→	1050 ←—→	820 ←—→ 600
Position[a], cm	3	12	18 23
Major elements	Si, C	Si, O	Si, O
Phases	SiO_xC_y, SiC	SiO_2, Si	SiO_2, Si
Morphology	Thin film	Whiskers	Spheroids

[a] Distance away from sample chamber.

3.2.3. FTIR analysis

FTIR diffuse reflectance spectra of the different deposits have been obtained, as shown in Fig. 6(a), (b) and (c), respectively. The thin film had one absorption peak at 810 cm^{-1} which is due to the stretching modes [23–25] of Si–C bond. The whiskers had four absorption peaks at 1160, 1070, 805 and 470 cm^{-1}; these closely resemble the SiO_2 glass whose peak positions [26,27] are 1080, 800 and 460 cm^{-1}. Pultz [28] observed two absorption peaks at 1165 and 1089 cm^{-1} belonging to amorphous SiO_2 which came from oxygenizing SiC fibers above 1000°C. Moreover, the crystalline varieties of SiO_2 such as quartz, cristobalite, or tridymite, yield a substantially sharper band [29], so whiskers deposits consist of amorphous SiO_2. The spectrum in Fig. 6(c) represents the spheroids which have two broad peaks appearing at 840–1300 cm^{-1} and 400–600 cm^{-1}. The former shows a prominently broader peak that may be attributed to the stretching modes of lattice vibration [30] involving Si–O–M, in which M = Si, Al or Ti, while the latter indicates the bending modes [30] of Si–O–M, in which M = Si or Al. Although the spheroids and whiskers deposits had the same components, they differed in terms of particle morphology, size and thickness, which ultimately shifted and changed the shape of IR absorption peaks [31–34]. After the three kinds of deposits had been leached by 10% HF solution for 24 h, the 810 cm^{-1} absorption peak of the thin film still obtained, but the absorption peaks of the whiskers and spheroids all disappeared. Hence, DRIFT spectra show that the thin film deposit has SiC, also the whiskers and spheroids deposits have a component of amorphous SiO_2.

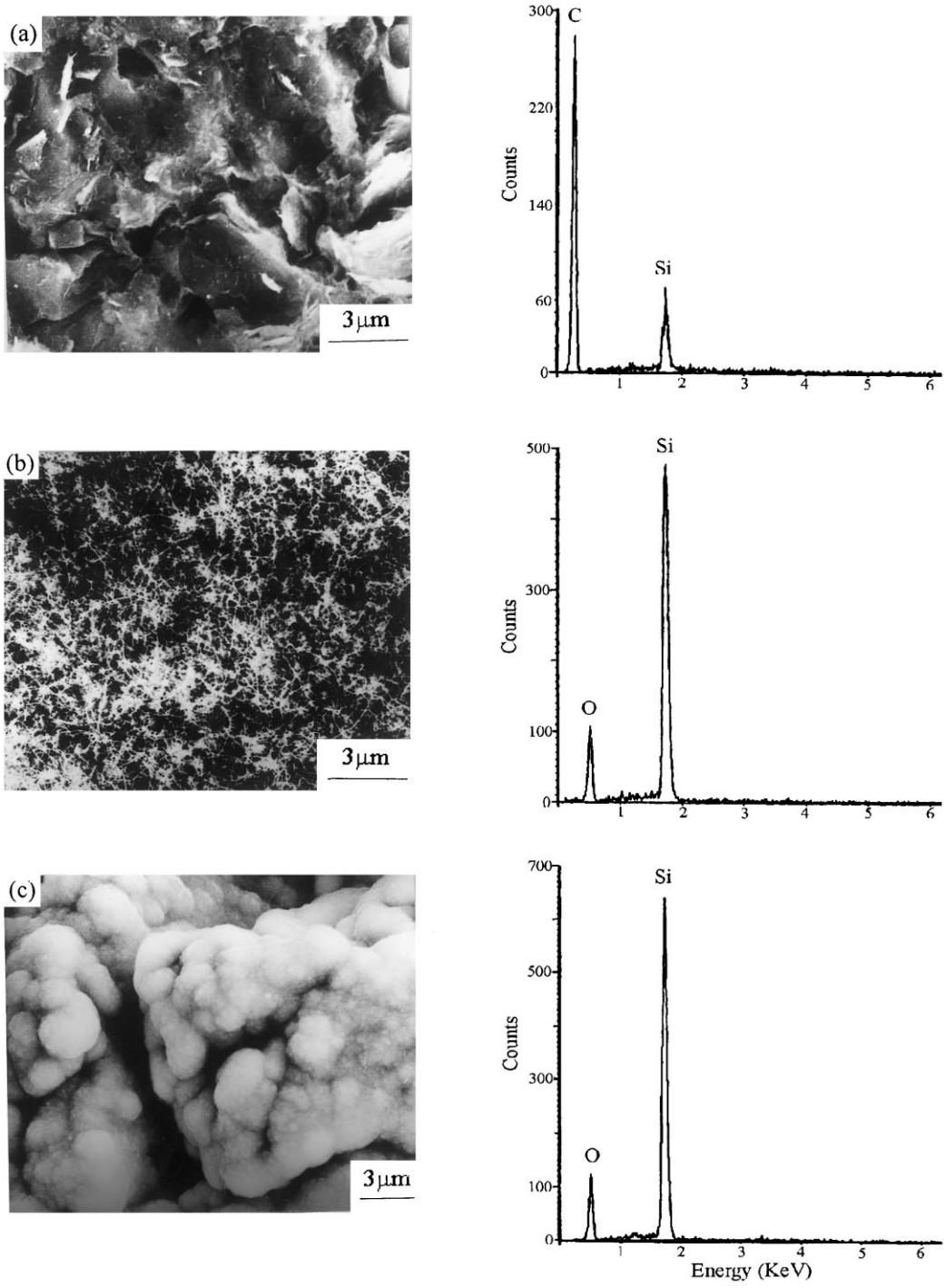

Fig. 3. SEM micrographs and EDS analysis of (a) the thin film, (b) whiskers, and (c) spheroids deposits on graphite substrates.

3.2.4. Surface analysis by XPS (ESCA) and AES

Electron spectroscopy for chemical analysis XPS has been considered to be useful for determining the chemical state (chemical binding energy and valency) of SiC surfaces in some previous studies [35,36]. Table 2 summarizes XPS analysis results for silicon (Si 2p) of different deposits on the graphite substrates. The thin film had two binding energies (Si 2p) of 101.8 eV for the most intense and 103.2 eV for the weak intense. The binding energy of Si 2p in SiO_xC_y [37] is about 101.5 eV, whereas in SiO_2 [38] it is about 103 to 104 eV. Also, Taylor [35] and Karasek [36] showed that SiC whiskers may have a surface of SiO_2 or SiO_xC_y. When the thin film had been leached by 10% HF solution, the 101.8 eV (Si 2p) was obtained, but the 103.2 eV vanished. Therefore, according to XRD, FTIR and XPS results, the

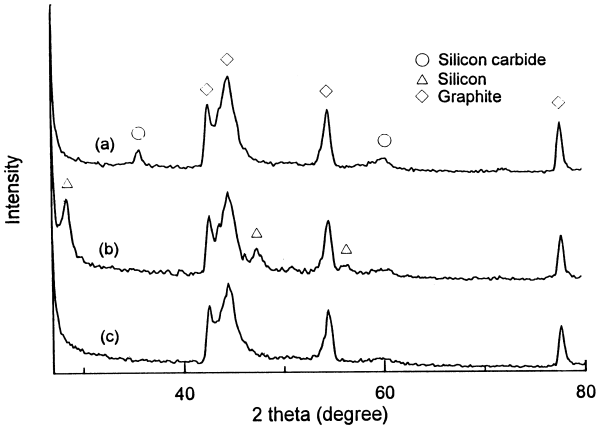

Fig. 4. Grazing incident X-ray diffractograms of (a) the thin film, (b) whiskers, and (c) spheroids deposits on graphite substrates.

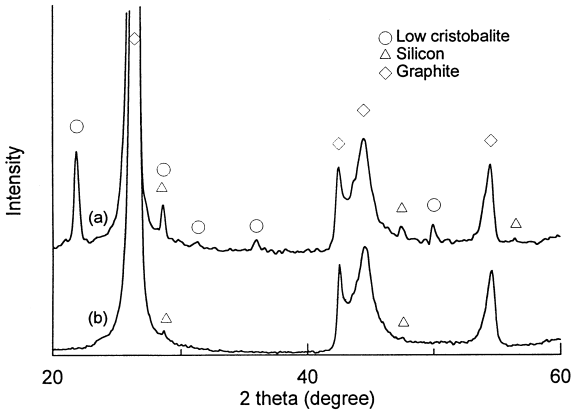

Fig. 5. X-ray diffractograms of spheroids deposits heat-treated at (a) 1000°C and (b) 1200°C in vacuum for 1 h.

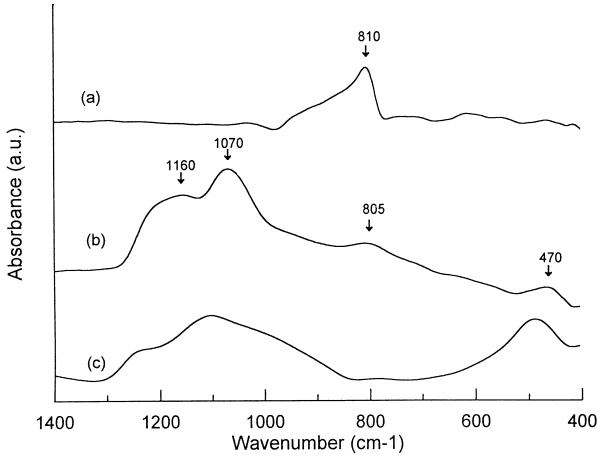

Fig. 6. FTIR diffuse reflection spectra of (a) the thin film, (b) whiskers, and (c) spheroids deposits on graphite substrates.

Table 2
Binding energy for Si 2p of different deposits in the cold zone by XPS

Zones	Morphology	Binding energy for Si 2p (eV)			
		Si	SiC	SiOC	SiO_2
Refs. [18,39]		99	100.2	101.5	103.7
A (1270–1050°C)	Thin film	–	–	101.8	103.2[a]
HF leached		–	–	101.3	–
B (1050–820°C)	Whiskers	98.8[a]	–	–	103.1
C (820–600°C)	Spheroids	98.8[a]	–	–	103.0

[a] Weak intensity.

thin film (SiC) was covered by an oxide layer, presumably SiO_xC_y. It was so thin that it couldn't be detected oxide elements by EDS. Shimokawa [18] in his study indicated that SiO_xC_y is a gradient material by the mixed compositions of SiO_2 and SiC.

Notably, the Si(2p) binding energies were 98.8, 103.1 eV and 98.8, 103.0 eV for the whiskers and spheroids, respectively. In solid silicon [39] the Si(2p) is about 99 eV. So, XPS results confirm that the surface of whiskers and spheroids both have Si and SiO_2 components which came from SiO by a decomposition process [Eq. (5)]. This is similar to the situation for the production of SiC in the Acheson [40] process, in which the outer core of the reacting pile contains significant quantities of silicon grains.

A surface depth profile analysis by AES was performed on the thin film that had been leached by HF solution. The results are shown in Fig. 7, indicating that SiC is present and the surface of SiC has an oxide layer (SiO_xC_y). Apparently, SiC appears to be a chemical gradient material on graphite substrate because Si and C elements varied in inverse proportions. Thus, AES analysis confirms the existence of the XPS results of the thin film.

According to the above results, when SiO and CO gases are released from CRH in the reaction zone (1300°C) and flow into the cold zone (1270–600°C) of the furnace tube, the vapour deposited products on graphite substrates are obtained as follows: in zone A, SiO may initially react with CO to form SiO_xC_y [18] and, then, SiO_xC_y continues to react with graphite to produce SiC on the graphite substrates. Therefore, in this zone, SiC is covered with SiO_xC_y. When these gases flow over the zone B and C (1050°C), SiC cannot form, possibly due to an energy barrier. Apparently, SiO gas is absorbed on the surface of substrates and decomposed to Si and SiO_2. The temperature of zone B exceeds the crystallization temperature of Si and, therefore, Si is crystallized in this zone. In brief, the deposits are crystalline Si and amorphous SiO_2 in zone B, as well as amorphous Si and SiO_2 in zone C. The sequence of morphology development of vapour deposited products with the decrease of temperature is: thin film (SiO_xC_y/SiC) →whiskers (Si/SiO_2)→spheroids (Si/SiO_2). This sequence is possibly related to the gases supersaturation and substrates temperature at the different zones, as shown

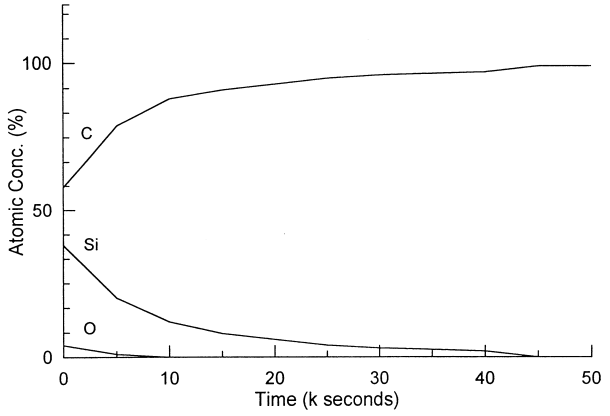

Fig. 7. AES depth profile of the thin film deposits after HF leaching.

by Blocher [41] in his studies of the structure/property/process relations in chemical vapour deposition (CVD). The deposits may adequately protect graphite substrates against erosion and oxidation, which can increase the commercial benefits of SiC synthesis from CRH.

4. Conclusion

The vapour deposited products on graphite substrates in the cold zone (1270–600°C), away from CRH in reacting sample chamber (1300°C), have been shown to give different morphologies and surface textures of the deposits. Characterization of these products gave the following results: in zone A (1270–1050°C), a thin film of SiC with an outer oxidized surface of SiO_xC_y was displayed; in zone B (1050–820°C), whiskers aggregates of crystalline Si together with amorphous SiO_2 were present; and in zone C (820–600°C), spheroid aggregates of amorphous Si and SiO_2 were obtained.

Morphologies of deposits on graphite substrates can be expressed by the following sequence with decreasing temperature: thin film (SiO_xC_y/SiC)→whiskers (Si/SiO_2)→spheroids (Si/SiO_2). The morphology sequence appears to be related to substrate temperature and supersaturation degree of the SiO gas in the cold zone of the tube furnace.

Further investigations on these different by-products coming from SiC formation from CRH, e.g. SiO_xC_y/SiC thin film, Si/SiO_2 whiskers and Si/SiO_2 spheroids, may possibly show their potential for various industrial applications.

Acknowledgements

The authors deeply thank Professors F.S. Yen, S.B. Wen, Dr. C.Y. Huang and Dr.Y.S. Hsu for their assistance and suggestions in this paper, and greatly appreciate the financial support of the National Science Council, R.O.C.

References

[1] J.V. Milewski, J.L. Sandstrom, W.S. Brown, Production of SiC from rice hulls, Silicon Carbide—1973, University of South Carolina Press, Columbia, 1974, pp. 634–639.
[2] J.G. Lee, I.B. Culter, Formation of SiC from rice hull, Am. Ceram. Bull. 54 (1975) 195–198.
[3] N.A.L. Mansour, S.B. Nanna, Silicon carbide and nitride from rice hulls 2. Effect of iron on the formation of silicon carbide, Brit. Ceram. Trans. J. 68 (1979) 132–136.
[4] M. Patel, A. Karera, Effect of fluxing agents in formation of SiC whisker from rice husk, Silicates Industrials 3/4 (1990) 103–105.
[5] R.V. Krishnarao, Formation of SiC whiskers from rice husk silica–carbon black mixture: effect of preheat treatment, J. Mater. Sci. Lett. 12 (1993) 1268–1271.
[6] R.V. Krishnarao, J. Subrahmanyam, Formation of SiC from rice husk silica–carbon black mixture: effect of rapid heating, Ceramics International 22 (1996) 489–492.
[7] S.N. Lakiza, Y.P. Dypan, Preparation of silicon carbide from rice husks, Sov. Powder Metall. Metal Ceram., English Translation 21 (1982) 117–121.
[8] R.V. Krishnarao, Effect of cobalt chloride treatment on the formation of SiC from burnt rice husks, J. Europ. Ceram. Soc. 12 (1993) 395–401.
[9] B.K. Padhi, C. Patnaik, Development of Si_2N_2O, Si_3N_4 and SiC ceramic materials using rice husk, Ceramics International 21 (1995) 213–220.
[10] R.V. Krishnarao, Effect of acid treatment on the formation of SiC whiskers from raw rice husks, J. Europ. Ceram. Soc. 15 (1995) 1229–1234.
[11] S.R. Nutt, Defect in SiC whiskers (rice hulls), J. Am. Ceram. Soc. 67 (6) (1984) 428.
[12] S.R. Nutt, Microstructure and growth model for rice-hull-derived SiC whiskers, J. Am. Ceram. Soc. 71 (3) (1988) 149–156.
[13] M. Patel, SiC from rice husk: ESCA studies, pmi. 22 (6) (1990) 31–33.
[14] M. Patel, A. Karera, SiC whiskers from rice husk: role of catalysts, J. Mater. Sci. Lett. 8 (1989) 955–956.
[15] M. Patel, A. Karera, SiC whisker from rice husk: microscopic study, pmi. 23 (1) (1991) 30–32.
[16] N.K. Sharma, W.S. Williams, Formation and structure of silicon carbide whiskers from rice hulls, J. Am. Ceram. Soc. 67 (11) (1984) 715–720.
[17] F. Viscomi, L. Himmel, Kinetic and mechanistic study on the formation of SiC from silica flour and coke breeze, J. Metals June (1978) 21–24.
[18] K. Shimokawa, I. Sekiguchi, Y. Ueda, Synthesis of ceramic fibers in the Si–O–C system, J. Ceram. Soc. Japan, Int. Edn 99 (1991) 741–746.
[19] K. Shimokawa, I. Sekiguchi, Y. Ueda, Synthesis of Si–O–C fibers from rice husk carbide—explanation of formation condition, J. Ceram. Soc. Japan, Int. Edn 100 (1992) 1111–1117.
[20] C.R. Blanchard, S.T. Schwab, X-ray diffraction analysis of the pyrolytic conversion of perhydropolysilazane into silicon nitride, J. Am. Ceram. Soc. 77 (7) (1994) 1729–1739.
[21] U. Ekhult, T. Carlberg, Oxygen solubility in liquid silicon in equilibrium with SiO and SiO_2, J. Electrochem. Soc. 136 (2) (1989) 551–554.
[22] N.A. Toropov, V.P. Barzakovskii, High-Temperature Chemistry of Silicates and Other Oxide Systems, Translated from Russian, Consultants Bureau, Plenum Publishing Corp., New York, 1966, pp. 115–140.
[23] A. Tsung, Y. Uwamino, T. Ishizuka, Determination of SiO_2 in SiC by diffuse reflectance infrared Fourier transform spectrometry, Applied Spectroscopy 40 (3) (1986) 310–313.
[24] J.F. DiGregorio, T.E. Furtak, Characterization of SiC whiskers through infrared absorption spectroscopy, J. Appl. Phys. 73(12) (1993) 8506–8513.

[25] M. Falk, S. Karunanithy, Determination of SiO_2 in SiC whiskers by infrared absorption spectroscopy, Mater. Sci. Eng. A114 (1989) 209–212.
[26] J.K. West, L.L. Hench, Molecular orbital models of silica rings and vibrational spectra, J. Am. Ceram. Soc. 78 (4) (1995) 1093–1096.
[27] W.A. Pliskin, Comparison of properties of dielectric films deposited by various methods, J. Vac. Sci. Technol. 14 (5) (1997) 1064–1081.
[28] W.W. Pultz, W. Hertl, Perturbations in the infrared spectra of submicroscopic size, single crystal, fibrous SiC, Spectrochimica Acta 22 (1966) 573–575.
[29] E. Dowty, Vibrational interactions of tetrahedral in silicate glasses and crystals: II. Calculations on melilites, pyroxenes, silica polymorphs and feldspars, Phys. Chem. Minerals 14 (1987) 122–138.
[30] S.K. Chen, H.S. Liu, C.S. Wu, Quantitative analysis of sphene and wollastonite crystallizations in annealed ceramics frits by FT-IR absorption spectroscopy, Applied Spectroscopy 47 (7) (1993) 965–972.
[31] W.M. Tuddenham, R.J.P. Lyon, Infrared techniques in the identification and measurement of minerals, Analytical Chemistry 32 (12) (1960) 1630–1634.
[32] M.P. Fuller, P.R. Griffiths, Diffuse reflectance measurements by infrared fourier transform spectrometry, Analytical Chemistry 50 (13) (1978) 1906–1910.
[33] G.R. Hunt, Infrared spectral behavior of fine particulate solids, J. Phys. Chem. 80 (11) (1976) 1195–1198.
[34] I.W. Boyd, J.I.B. Wilson, Silicon–silicon dioxide interface: an infrared study, J. Appl. Phys. 62(8) (1987) 3195–3199.
[35] T.N. Taylor, The surface composition of SiC powders and whiskers: an XPS study, J. Mater. Res. 4 (1) (1989) 189–203.
[36] K.R. Karasek, J.L. Schienle, Characterization of recent SiC whiskers, J. Mater. Sci. 26 (1991) 103–111.
[37] G.M. Renlund, S. Prochazka, Silicon oxycarbide glasses: Part 2. Structure and properties, J. Mater. Res. 6 (12) (1991) 2723–2734.
[38] M.N. Rahaman, L.C. De Jonghe, Angle-resolved XPS analysis of oxidized polycrystalline SiC surfaces, Am. Ceram. Soc. Bull. 66 (5) (1987) 782–785.
[39] C.D. Wagner, W.M. Riggs, G.E. Muilenberg, Handbook of X-ray Photoelectron Spectroscopy, Perkin-Elmer Corp., Eden Prairie, MN, 1979, p. 52.
[40] V. Haase, H. Vanecek, Gmelin Handbook of Inorganic Chemistry, 8th ed., supplement vol. B3, Springer-Verlag, Berlin, 1985, pp. 53–61.
[41] J.M., Jr. Blocher, Structure/property/process relationship in chemical vapour deposition CVD, J. Vac. Sci. Technol. 11 (4) (1974) 680–686.